

Conformational Properties of Poly(vinylidene fluoride). A Quantum Chemistry Study of Model Compounds

Oleksiy G. Bytner and Grant D. Smith*

Department of Materials Science and Engineering and Department of Chemical and Fuels Engineering, 122 S. Central Campus Drive Rm. 304, University of Utah, Salt Lake City, Utah 84112

Received February 23, 1999; Revised Manuscript Received August 25, 1999

ABSTRACT: The molecular geometries and conformational energies of model molecules of poly(vinylidene fluoride) (PVDF) have been determined from high-level quantum chemistry calculations and have been used in parametrization of a six-state rotational isomeric state (RIS) model for PVDF. The model molecules investigated were 1,1,1,3,3-pentafluorobutane, 1,1,1,3,3,5,5,5-octofluoropentane, 2,2,4,4-tetrafluoropentane, and 2,2,4,4,6,6-hexafluoroheptane (HFH). Analysis of the conformations of these molecules revealed split trans minima ($t_+ = 195^\circ$, $t_- = 165^\circ$), as was seen in previous studies of perfluoroalkanes. In contrast, the gauche minima, which split in perfluoroalkanes, did not do so in the PVDF model compounds. The lowest energy conformer of HFH, $g^+g^+g^+g^+$, was found to be at least 0.4 kcal/mol lower in energy per backbone dihedral than any of the conformers of HFH resembling crystalline polymorphs of PVDF, indicating that intermolecular interactions are important in stabilizing conformations of PVDF in the crystalline phases. A six-state RIS model was able to accurately reproduce the conformer energies of the PVDF model compounds. The RIS analysis revealed that, as in *n*-alkanes and perfluoroalkanes, the trans conformation of the backbone dihedral is intrinsically lower in energy than the gauche conformation in the PVDF model compounds. However, very large unfavorable second-order interactions between fluorine atoms occur in $-\text{CH}_2-$ centered t_+t_+ sequences and, to a lesser extent, t_+g^+ and t_+g^- sequences. The quantum chemistry based RIS model yielded a characteristic ratio for PVDF in good agreement with experiment, but with significantly different conformer populations than predicted by earlier RIS models, including a much higher gauche probability. The high gauche probability of 65% for unperturbed PVDF chains (at 463 K), greater than that for poly(ethylene) and much greater than that for poly(tetrafluoroethylene), is a consequence of the unfavorable second-order interactions occurring in $-\text{CH}_2-$ centered sequences containing trans conformations.

Introduction

Poly(vinylidene fluoride) (PVDF) is a technologically important semicrystalline polymer. It has at least four crystalline polymorphs with relatively high melting temperatures ranging from 160 to 180 °C.¹ Four crystal structures of PVDF have been well-studied using various crystallographic techniques including X-ray diffraction, wide-line NMR, and Raman spectroscopy.^{2–5}

Much of the interest in crystalline PVDF stems from its extraordinary piezoelectric and pyroelectric properties that were first reported by Kawai⁶ in 1969 and Bergman et al.⁷ in 1971. Both properties result from the macroscopic polarization that may be imparted to PVDF samples by drawing of extruded thin films.⁸ The piezoelectric properties of PVDF have been exploited widely in technical applications.⁹ The properties of amorphous PVDF are also of great interest, as PVDF constitutes the major component in a variety of amorphous fluoroelastomers such as Viton. Fluoroelastomers are fluorine-containing high-performance synthetic rubbers that have exceptional resistance to a broad spectrum of oils, gases, fluids, and chemicals at elevated temperatures and severe environments. They are partially fluorinated or perfluorinated alkanes randomly copolymerized with bulky comonomers such as hexafluoropropylene in order to reduce or prevent crystallization. PVDF and its copolymers are also being explored as major components in electrolyte membranes for secondary lithium battery and fuel cell applications.

In an effort to better understand the conformational characteristics of PVDF and the influence of condensed-phase interactions on PVDF conformations, we have performed ab initio electronic structure calculations on model PVDF compounds and have developed a rotational isomeric state (RIS) model for PVDF on the basis of these studies. In the next section we describe the methods and results of ab initio quantum chemistry calculations made on PVDF model molecules. These calculations provide the geometry and conformational energy data required for the parametrization of an RIS model for PVDF. In section III we present the quantum chemistry based RIS model for PVDF and compare predictions of the conformer energies of the PVDF model compounds with quantum chemistry. In addition, predicted polymer properties are compared with available experimental data, and the present quantum chemistry based RIS model is compared with those derived previously for PVDF as well as polyethylene (PE) and poly(tetrafluoroethylene) (PTFE). In an upcoming paper, we will present a classical force field for PVDF based upon the quantum chemistry and RIS studies of the PVDF model compounds and will consider the properties of PVDF melts from molecular dynamics simulations.

Quantum Chemistry Studies

Level of Theory. The model molecules 1,1,1,3,3-pentafluorobutane (PFB), 1,1,1,3,3,5,5,5-octofluoropentane (OFP), 2,2,4,4-tetrafluoropentane (TFP), and 2,2,4,4,6,6-hexafluoroheptane (HFH), shown in Figure 1 in all-trans conformations, were studied. Here, trans (*t*) corresponds to a dihedral angle of 180°. All quantum

* To whom correspondence should be addressed.

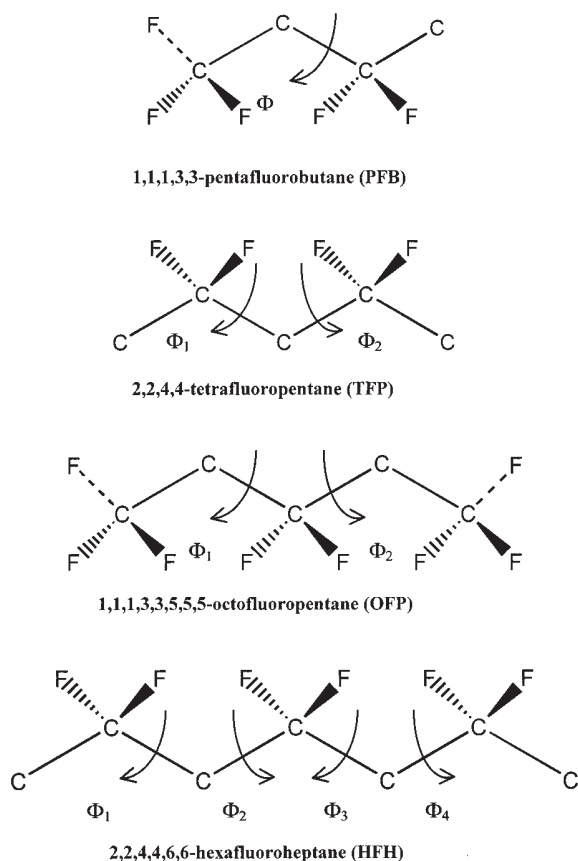


Figure 1. Model compounds for poly(vinylidene fluoride). Hydrogen atoms are not shown. Backbone dihedrals are indicated.

Table 1. Conformational Geometries and Energies^a of 2,2,4,4-Tetrafluoropentane (TFP)

conformer ^b	type	ϕ_1 (deg)	ϕ_2 (deg)	D95+**		D95+(2d,p)	
				SCF	MP2	SCF	MP2
g^+g^+	min	58.7	58.7	0.00	0.00	0.00	0.00
g^+g^+c	min	56.8	56.8	0.00	0.00	0.00	0.00
g^+t-	min	50.3	167.9	0.73	0.91	0.68	0.94
g^+g^-	min	50.8	-86.7	3.43	3.14	3.30	3.14
t_+t_+	min	193.2	193.2	3.10	3.63	2.88	3.46
t_+t_+c	min	195.8	195.8	3.04	3.70	2.81	3.53
$g^+t_-g^+g^+$	saddle ^d	65.8	120.3	3.41	3.52	3.49	3.64
$g^+g^-g^-g^+g^-$	saddle ^e	66.3	-66.3	3.68	3.83	3.74	3.79
<i>tcis</i>	saddle ^d	180.0	0.0	3.80	3.83	3.89	3.87
$t_-t_-t_-g^+$	saddle ^d	178.9	124.4	5.09	5.46	4.99	5.45
<i>tt</i>	saddle ^d	180.0	180.0	3.25	3.93	3.01	3.79
<i>tt</i> ^c	saddle	180.0	180.0	3.18	4.13	2.90	3.89
g^+t_+	not found						
t_+t_-	not found						

^a Relative to the g^+g^+ conformer in kcal/mol. ^b SCF/D95** geometry. ^c MP2/D95** geometry. ^d Saddle point of the first order. ^e Saddle point of the second order.

chemistry calculations were performed using the quantum chemistry package Gaussian 98.¹⁰ Geometry optimizations were performed at the SCF/D95** level and at the MP2/D95** level for selected TFP conformers. As shown in Table 1, geometry optimization at the MP2 level makes little difference in the conformational geometries or subsequent single-point SCF and MP2 energies. Therefore, only the much less computationally expensive SCF geometries were determined for the remaining TFP conformers and for the other compounds investigated.

Table 2. Conformational Geometries and Energies^a of 1,1,1,3,3-Tetrafluorobutane (PFB)

conformer ^b	type	ϕ (deg)	D95+**		
			SCF	D95+** SCF	D95+** MP2
g^+	minimum	53.4	0.00	0.00	0.00
t_+	minimum	175.3	1.14	1.08	1.47
<i>t</i>	saddle	180.0	1.15	1.07 ^c	1.49
<i>cis</i>	saddle	0.0	3.24	3.12	2.90
g^+t	saddle	122.9	3.28	3.28	3.42
g^+_+	not found ^d				

^a Relative to the g^+ conformer, in kcal/mol. ^b SCF/D95** geometries. ^c The fact that this energy is lower than that of the t_+ conformer is a consequence of using D95** geometries with D95+** energies. For D95+** geometries, *t* is a saddle point. ^d An extensive search for split gauche states was performed. The dihedral was constrained to a series of possible values for the split gauche, with geometry optimization for the remaining degrees of freedom. Full geometry optimizations were then performed. In each case the molecule returned to one of the 6-31G** and D95** basis sets using analytical second derivatives.

Table 3. Conformational Geometries and Energies^a of 1,1,1,3,3,5,5,5-Octofluoropentane (OFP)

conformer ^b	type	ϕ_1 (deg)	ϕ_2 (deg)	D95+**	
				SCF	MP2
g^+g^+	min	62.2	62.2	0.00	0.00
g^+t_-	min	54.2	165.5	0.76	1.46
g^+g^-	min	61.1	-109.3	3.59	3.44
<i>tt</i>	min	180.0	180.0	2.13	3.70
$g^+t_-g^+g^+$	saddle ^c	69.1	118.4	3.26	3.99
<i>tcis</i>	saddle ^c	180.0	0.0	4.20	4.81
$t_-t_-t_-g^+$	saddle ^c	175.8	123.2	4.19	5.41
t_+t_+	not found				

^a Relative to the g^+g^+ conformer in kcal/mol. ^b SCF/D95** geometry. ^c Saddle point of the first order.

Diffuse functions proved to have an important influence on the relative conformer energies in perfluoroalkanes¹¹ and perfluoroethers.¹² Consequently, we augmented the basis set for the PVDF model compounds to D95+** for single-point energy calculations. The effects of basis set size and electron correlation on relative conformer energies were investigated for TFP, as shown in Table 1. Augmentation of the D95+** basis set with additional polarization functions made little difference in the relative conformer energies with the exception of the *tt* saddle point. In contrast, MP2 energies differ significantly from SCF values for many of the more important (lower energy) conformers of the PVDF model compounds (see also Tables 2 and 3). These results are consistent with those previously obtained for perfluoroalkanes¹¹ and perfluoroethers.¹² Consequently, we concluded that calculations on PVDF model compounds performed at the SCF/D95**//MP2/D95+** geometry/energy level should yield accurate relative conformational energies.

Butane Compound. The conformational energies and geometries of PFB, the shortest model compound studied, are strongly influenced by the terminal CF₃ and CH₃ groups, which are not important in PVDF and its higher molecular weight oligomers. As these end effects may dominate in PFB, the conformational energetics and geometries of this compound are relatively unimportant in elucidating the properties of PVDF. However, we found it useful to study the compound and compare conformational properties with those of the equivalent compound for PTFE, perfluorobutane (PerFB).

The conformational energies and geometries of PFB are given in Table 2. In addition to the SCF/D95**//MP2/

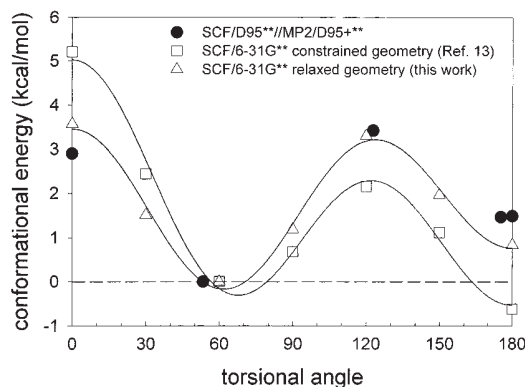


Figure 2. Conformational energy of 1,1,1,3,3-pentafluorobutane (PFB) as a function of dihedral angle. The lines serve to guide the eye.

D95** calculations, results of SCF/6-31G** level calculations are shown in Figure 2 for comparison with a previous quantum chemistry study of PFB.¹³ That study constitutes the only ab initio calculations on model compounds for PVDF that we were able to find in the literature. In that study, a full geometry optimization was performed at the SCF/6-31G** level for PFB with the backbone dihedral constrained to 180°. A rigid rotation of the dihedral at 30° intervals was performed without allowing the valence geometry to relax. Single-point energies were determined at these new geometries. Unfortunately, constraining the valence geometry to that obtained for the $\phi = 180^\circ$ conformer significantly influences the relative conformer energies. This can be seen by examining Figure 2, where a comparison of the relative conformer energies obtained in ref 13 is made with those obtained by constraining the backbone dihedral but allowing the valence geometry to relax. The conformational picture obtained in ref 13 is qualitatively incorrect. This can be seen clearly in Figure 2, which shows that the lowest energy conformer for relaxed geometries is gauche instead of trans.

It is instructive to compare the conformational energetics of PFB with those previously obtained for perfluorobutane (PerFB).¹¹ PerFB has split trans minimum with the 180° backbone dihedral corresponding to a saddle point between the t_+ and t_- minima. Note that while the splitting is weak in PFB, it is much stronger in the longer PVDF model compounds which are more representative of the polymer. In contrast to PerFB, PFB does not exhibit a split gauche conformer. In addition, while the t_+ (or the equivalent t_-) conformer is almost 0.5 kcal/mol lower in energy than the gauche conformer in PerFB, Table 2 reveals that the gauche conformer is the lowest energy conformer in PFB by nearly 1.5 kcal/mol. This effect can be associated with the relief of unfavorable F–F steric and electrostatic interactions manifested in the PFB t_+ conformer and favorable F–H electrostatic interactions manifested in the PFB g^+ conformer, as illustrated in Figure 3. In PerFB, the methyl group is replaced by a trifluoromethyl group, and consequently the gauche arrangement is both sterically and electrostatically less favorable than in PFB.

Pentane Compounds. The relative energies and conformational geometries for the conformers and rotational energy barriers for the $-\text{CH}_2-$ centered pentane model compound, TFP, are given in Table 1, while the same are given for the $-\text{CF}_2-$ centered pentane model compound, OFP, in Table 3. Again, it is instruc-

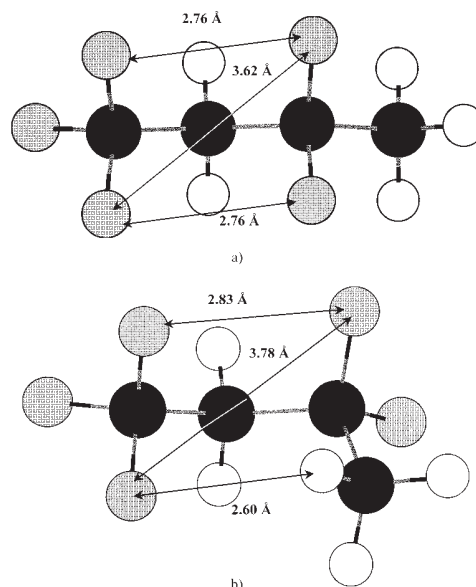


Figure 3. Comparison of interatomic interactions in 1,1,1,3,3-pentafluorobutane (PFB) for (a) t_+ and (b) g^+ conformers. Important interatomic distances are indicated.

tive to compare results for these compounds with our previous study of the perfluorinated analogue, perfluoropentane (PerFP).¹¹ We can see the split trans state in TFP and OFP, and as in PerFP, the t_+t_- conformation does not correspond to a stationary point. As in PFB, after a careful search for another minimum near the gauche state in TFP and OFP, we could not find any evidence for a split gauche state in these compounds. This is in contrast to PerFP, which exhibits split gauche states. The conformers with gauche states of opposite sign manifest the pentane effect, and as is typically seen, one of the gauche dihedrals is significantly distorted. These distorted states are given labels g^+g^- and g^-g^+ . The g^+g^- energy is relatively high (3.14 kcal) although it is lower by 0.5 kcal than the t_+t_+ conformer. It is also worth noting that while g^+t_+ type conformers are found in PerFP (albeit higher in energy than the preferred g^+t_- conformers), the corresponding conformers were not found in TFP or OFP.

Heptane Compound. The relative energies and conformational geometries for selected low-energy conformers and rotational energy barriers of HFH are given in Table 4. The lowest energy conformer of HFH is $g^+g^+g^+g^+$, consistent with results for the butane and pentane compounds. The all-trans planar zigzag conformation, which corresponds to the conformer of PVDF in the β -crystal polymorph,^{2,13} is a saddle point and lies 7.5 kcal/mol, or more than 1.8 kcal/mol per backbone dihedral, higher in energy than the $g^+g^+g^+g^+$ conformer. The $g^-t_+g^+t_-$ HFH conformer is similar in geometry to the sequence $TGT\bar{C}$ found for the α and δ polymorphs of PVDF^{3,4,13} and lies only about 0.4 kcal/mol per backbone dihedral above the global minimum $g^+g^+g^+g^+$. The final PVDF polymorph, the γ form, has a conformational sequence $T_3GT_3\bar{C}$.^{3,13} The HFH conformer $t_-t_-t_-g^+$, with an energy of 3.5 kcal/mol, or about 0.9 kcal/mol per backbone dihedral above the global minimum, is similar in geometry to half of this sequence. These comparisons indicate that strong condensed phase effects are manifested in crystalline PVDF. From the dipole moments given in Table 4 for the HFH conformers, it can be seen that the conformers resem-

Table 4. Conformational Geometries and Energies^a of 2,2,4,4,6,6-Hexafluoroheptane (HFH)

conformer ^b	type	ϕ_1 (deg)	ϕ_2 (deg)	ϕ_3 (deg)	ϕ_4 (deg)	D95+** MP2	DM ^c
$g^+g^+g^+g^+$	min	65.3	65.1	65.1	65.3	0.00	2.36
$g^+g^+t_+g^-$	min	53.9	62.0	188.4	-50.8	0.27	1.68
$g^+g^+t_-g^+$	min	60.6	59.3	164.0	50.6	0.33	2.83
$g^+g^+g^+t_+$	min	64.0	61.2	66.6	187.2	0.48	2.92
$t_+g^+g^+t_-$	min	194.0	69.8	52.4	171.9	0.62	2.45
$g^+t_-g^+t_-$	min	51.3	165.5	51.1	168.0	0.81	3.75
$g^+t_-t_-g^+$	min	50.9	166.0	166.0	50.9	1.21	0.01
$g^-t_+g^+t_-$	min	-51.4	184.2	52.4	165.0	1.55	4.42
$g^+g^+t_+t_+$	min	55.7	62.9	190.4	193.4	2.29	2.25
$t_-t_-g^+t_-$	min	165.9	163.7	50.4	167.2	2.93	4.21
$g^-g^+t_-g^+$	min	-87.2	52.3	165.7	50.6	3.09	1.88
$g^+t_-t_-t_-$	min	50.0	165.5	164.0	165.8	3.52	3.66
$t_-t_-t_-t_-$	min	165.7	163.9	163.9	165.7	6.53	6.44
$tttt^d$	saddle	180.0	180.0	180.0	180.0	7.51	6.84

^a Relative to the $g^+g^+g^+g^+$ conformer, in kcal/mol. ^b SCF/D95** geometries. ^c Dipole moment, in debyes, from SCF/D95+** wave functions. ^d Dihedral angles were constrained at their indicated values.

bling sequences found in the crystal polymorphs of PVDF have large dipole moments. In contrast, the $g^+g^+g^+g^+$ conformer has a relatively small dipole moment. It is likely that intermolecular polar interactions stabilize the conformers of PVDF found in the various polymorphs.

It should also be noted that both $-CH_2-$ and $-CF_2-$ centered g^+t_+ sequences are found in HFH. These sequences are not observed in the pentane model compounds but are seen in perfluoropentane. The absence of these sequences in the pentane PVDF model compounds may be due to chain end effects. Interactions involving the methyl and trifluoromethyl groups capping the model compounds may differ sterically and electrostatically from those involving $-CH_2-$ and $-CF_2-$ groups in the longer compounds.

Rotational Isomeric State Model

Model Compounds. Previously, we were able to accurately describe the relative energies of the low-energy conformers of perfluoroalkanes (butane, pentane, and hexane) obtained from quantum chemistry using a six-state RIS description that took into account the split trans and gauche states.¹¹ This model predicted conformational properties of PTFE in good agreement with experiment. For PE and *n*-alkanes, a five-state model, which includes distorted gauche states (g^+_{+} , g^-_{-}) that are manifested in pentane interactions ($g^-g^+_{+}$ and $g^-g^+_{-}$ sequences), has been successfully employed.^{14,15} For PVDF, six-state and three-state RIS models for PVDF have been developed.^{16,17} Below, these models will be compared with the quantum chemistry based model for PVDF presented here. Examination of Tables 1–4 and Figure 2 reveals that while the trans state is clearly split in the longer PVDF model compounds, the gauche states are not. As in PE, the pentane effect leads to highly distorted gauche states. We therefore determined that best RIS representation of the PVDF compounds could be obtained with a six-state model that has split trans states (as in PTFE) and pentane-effect-induced distorted gauche states (as in PE).

The RIS representation of the PVDF model compounds in terms of first (dependent upon one dihedral) and second (dependent upon consecutive dihedrals) interactions is given in Table 5. The energies associated with these interactions are given in Table 6. The six-

state model provides a reasonably accurate description of the conformational energies of all compounds. The description is best for the lowest energy HFH compounds, which were given the greatest weight in the fitting procedure. The first-order interaction, σ , manifested in the trans state (relative to the gauche state) has an energy E_{σ} of -0.50 kcal/mol. For the $-CH_2-$ centered dihedral pairs, the second-order interaction for t_+t_+ sequences, δ_H , is highly unfavorable, with $E_{\delta_H} = 3.95$ kcal/mol. The second-order interaction for $-CF_2-$ centered t_+t_+ sequences, δ_F , has an energy $E_{\delta_F} = 0.10$ kcal/mol. The second-order interactions resulting from $-CF_2-$ and $-CH_2-$ centered t_-g^+ sequences, ψ_F and ψ_H , respectively, have energies $E_{\psi_F} = -0.35$ kcal/mol and $E_{\psi_H} = 1.10$ kcal/mol. The second-order energies γ_F and γ_H , associated with t_-g^- sequences (which are not observed in pentane compounds but are found in HFH), are $E_{\gamma_F} = -0.25$ kcal/mol and $E_{\gamma_H} = 0.75$ kcal/mol, respectively. Hence, in HFH, t_-g^- sequences are quite similar in energy to the t_-g^+ sequences. Finally, the second-order pentane interactions arising in $-CF_2-$ and $-CH_2-$ $g^-g^+_{+}$ and $g^+g^-_{-}$ sequences are similar and can be accurately described by a single interaction ω with $E_{\omega} = 3.2$ kcal/mol.

Examination of the first-order and second-order interaction energies provides insight into the conformational characteristics of PVDF and its model compounds. The negative value for E_{σ} indicates that the trans state of the backbone dihedrals in the PVDF model compounds is intrinsically favored, as is found in perfluoroalkanes and *n*-alkanes. The large positive energy for the second-order interaction δ_H accounts for the high energy of $-CH_2-$ centered t_+t_+ sequences. As this sequence results in sterically and electrostatically strained F–F interactions, the large positive energy is reasonable. In contrast, for $-CF_2-$ centered pairs, the second-order interaction δ_F , which results in H–H interactions, is much more favorable. Because of relief of the F–F interactions, the second-order interactions in $-CH_2-$ tg sequences, ψ_H and ψ_H , are much more favorable than is found in t_+t_+ sequences (δ_H). The energies of the ψ_H and ψ_H interactions are still large and positive, however, indicative of unfavorable interactions relative to the g^+g^+ sequences. For the $-CF_2-$ tg sequences, the second-order interactions are small, i.e., similar to those arising in the g^+g^+ sequence.

On the basis of the above analysis, it can be seen that the t_+t_+ $-CF_2-$ centered sequence is actually lower in energy than the g^+g^+ sequence. Hence, we might expect t_+t_+ to be the preferred conformation of OFP. However, a t_+ conformation in OFP results in F–F interactions between a $-CF_2-$ group and a trifluoromethyl end group. Therefore, the t_+t_+ conformation of OFP involves two $-CH_2-$ centered δ_H -like interactions involving the trifluoromethyl end groups. A good representation of the energies of PFB and OFP, which manifest these interactions, was obtained by assigning these interactions an energy of $0.75E_{\delta_H}$ (see Table 5). As these interactions involve the relatively conformationally flexible trifluoromethyl groups, a second-order interaction somewhat more favorable than the δ_H interaction is reasonable. As a result of these very high-energy second-order interactions, the t_+t_+ conformation of OFP is much higher in energy than the g^+g^+ conformer, and the t_+ conformer of PFB is higher in energy than the g^+ conformer.

Table 5. RIS Representation of PVDF Model Compounds

conformer	first and second-order interactions								energy (kcal/mol)	
	σ	δ_F	δ_H	ψ_F	ψ_H	γ_F	γ_H	ω	QC	RIS
1,1,1,3,3-Pentafluorobutane (PFB)										
g^+	0	0	0	0	0	0	0	0	0.00	0.00
t_+	1	0	$3/4$	0	$-3/4$	0	0	0	1.47	1.65
2,2,4,4-Tetrafluoropentane (TFP)										
g^+g^+	0	0	0	0	0	0	0	0	0.00	0.00
g^+t_-	1	0	0	0	1	0	0	0	0.91	0.60
g^+g^-	0	0	0	0	0	0	0	1	3.1	3.2
t_+t_+	2	0	1	0	0	0	0	0	3.63	2.95
1,1,1,3,3,5,5-Octofluoropentane (OFP)										
g^+g^+	0	0	0	0	0	0	0	0	0.00	0.00
g^+t_-	1	0	$3/4$	1	$-3/4$	0	0	0	1.46	1.30
g^+g^-	0	0	0	0	0	0	0	1	3.4	3.2
t_+t_+	2	1	$3/2$	0	$-3/2$	0	0	0	3.70	3.40
2,2,4,4,6,6-Hexafluoroheptane (HFH)										
$g^+g^+g^+g^+$	0	0	0	0	0	0	0	0	0.00	0.00 (1.59) ^a
$g^+g^+t_+g^-$	1	0	0	0	1	1	0	0	0.27	0.35 (0.38)
$g^+g^+t_-g^+$	1	0	0	1	1	0	0	0	0.33	0.25 (0.38)
$g^+g^+g^+t_+$	1	0	0	0	0	0	1	0	0.48	0.25 (1.10)
$t_+g^+g^+t_-$	2	0	0	0	1	0	1	0	0.62	0.85 (1.25)
$g^+t_-g^+t_-$	2	0	0	1	2	0	0	0	0.81	0.85 (0.53)
$g^+t_-t_-g^+$	2	1	0	0	2	0	0	0	1.21	1.30 (0.00)
$g^-t_+g^+t_-$	2	0	0	0	2	1	0	0	1.55	0.95 (0.53)
$g^+g^+t_+t_+$	2	0	1	0	0	1	0	0	2.29	2.70 (0.69)
$t_-t_-g^+t_-$	3	0	1	1	1	0	0	0	2.93	3.20 (0.84)
$g^-g^+t_-g^+$	1	0	0	1	1	0	0	1	3.09	3.45 (0.62)
$g^+t_-t_-t_-$	3	1	1	0	1	0	0	0	3.52	3.65 (0.31)
$t_-t_-t_-t_-$	4	1	2	0	0	0	0	0	6.53	6.0 (1.25)

^a From the three-state RIS model of ref 16.

ϕ_i	t_+	t_-	g^+	g^+	g^-	g^-
ϕ_{i-1}						
t_+	$\sigma\delta_{F,H}$		$\gamma_{F,H}$	$\omega\gamma_{F,H}$	$\psi_{F,H}$	$\omega\psi_{F,H}$
t_-		$\sigma\delta_{F,H}$	$\psi_{F,H}$	$\omega\psi_{F,H}$	$\gamma_{F,H}$	$\omega\gamma_{F,H}$
g^+	$\sigma\gamma_{F,H}$	$\sigma\psi_{F,H}$	1	ω		ω
g^+	$\sigma\gamma_{F,H}$	$\sigma\psi_{F,H}$	1		1	
g^-	$\sigma\psi_{F,H}$	$\sigma\gamma_{F,H}$		ω	1	ω
g^-	$\sigma\psi_{F,H}$	$\sigma\gamma_{F,H}$	1		1	

Figure 4. Statistical weight matrices for poly(vinylidene fluoride).

Table 6. First-Order and Second-Order Energies (in kcal/mol) for the Six-State RIS Model of PVDF

E_σ	E_{δ_F}	E_{δ_H}	E_{ψ_F}	E_{ψ_H}	E_{γ_F}	E_{γ_H}	E_ω
-0.50	0.10	3.95	-0.35	1.10	-0.25	0.75	3.20

Statistical Weight Matrixes. The second-order statistical weight matrices for the $-CH_2-$ and $-CF_2-$ centered dihedral pairs are given in Figure 4. The statistical weight associated with each first- and second-order interaction μ is given as

$$\mu = F_\mu \exp(-E_\mu/kT) \quad (1)$$

where E_μ is the energy associated with the interactions (see Table 6), k is the Boltzmann constant, T is temperature, and F_μ is a preexponential, or entropic, factor. We assigned $F_\mu = 1$ for all interactions except for the first-order σ interaction and the second-order δ_H and δ_F interactions. We assigned $F_\sigma = 0.5$ in order to avoid over weighting t_+ and t_- states, since these state

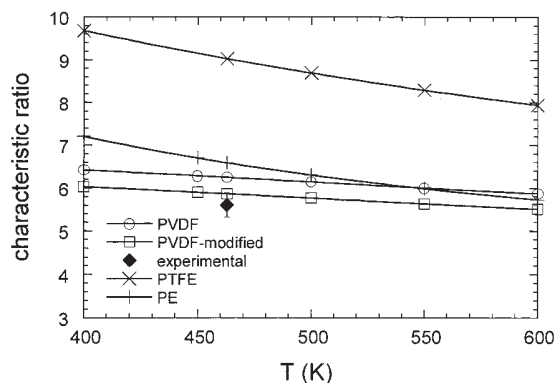


Figure 5. Characteristic ratio C_∞ of poly(vinylidene fluoride), polyethylene, and poly(tetrafluoroethylene) as a function of temperature. The modified PVDF values were determined using the experimental valence angles.

actually span only $1/2$ of the conformational space (60°) of a gauche state (120°). This results, however, in under weighting of tt states, as t_+t_- and t_-t_+ states are not allowed. Consequently, we assign $F_{\delta_H} = 2$ and $F_{\delta_F} = 2$. It should also be noted that while ω is a second-order interaction arising in g^+g^- type sequences, we consider the g^- states to exist only in these sequences, and hence ω is associated with each g^- and g^+ conformation in the statistical weight matrices.

Using standard techniques,¹⁸ we calculated the characteristic ratio C_∞ of unperturbed chains of PVDF using the statistical weight matrices given in Figure 4. C_∞ for PVDF is plotted as a function of temperature in Figure 5. We used backbone valence angles of 120° and 118° for the $-CF_2-$ and $-CH_2-$ centered angles, respectively. For the RIS states, we used dihedral angles of $t_+ = 195^\circ$, $t_- = 165^\circ$, $g^+ = 59^\circ$, $g^+ = 90^\circ$, $g^- = 301^\circ$, and $g^- = 270^\circ$. Valence and torsional angles were obtained from the quantum chemistry geometries of the

ϕ_i	t_+	t_-	g^+	g^+	g^-	g^-
ϕ_{i-1}						
t_+	0.009	0	0.093	0.004	0.064	0.003
t_-	0	0.009	0.064	0.003	0.093	0.004
g^+	0.093	0.064	0.139	0.006	0	0.006
g^+	0.004	0.003	0.006	0	0.006	0
g^-	0.064	0.093	0	0.006	0.139	0.006
g^-	0.003	0.004	0.006	0	0.006	0

a)

ϕ_i	t_+	t_-	g^+	g^+	g^-	g^-
ϕ_{i-1}						
t_+	0.029	0	0.065	0.003	0.073	0.003
t_-	0	0.029	0.073	0.003	0.065	0.003
g^+	0.065	0.073	0.156	0.007	0	0.007
g^+	0.003	0.003	0.007	0	0.007	0
g^-	0.073	0.065	0	0.007	0.156	0.007
g^-	0.003	0.003	0.007	0	0.007	0

b)

Figure 6. Populations of (a) $-\text{CH}_2-$ and (b) $-\text{CF}_2-$ centered dihedral pairs in poly(vinylidene fluoride) at 463 K from the quantum chemistry based RIS model.

low-energy PVDF model compounds. A value of $C_\infty = 5.6 \pm 0.3$ for PVDF has been found in benzophenone at Θ conditions (463 K) by employing a combination of viscosity and light-scattering measurements.¹⁹ Our value of $C_\infty = 6.22$ at 463 K using the quantum chemistry based RIS model and quantum chemistry geometries, without modification, is in reasonable agreement with experiment. If we employ values of 118.5° and 116.5° for the $-\text{CF}_2-$ and $-\text{CH}_2-$ centered angles, respectively, as obtained from X-ray crystallographic studies of PVDF,² we obtain a value of $C_\infty = 5.86$, in good agreement with experiment.

The populations of the $-\text{CH}_2-$ and $-\text{CF}_2-$ centered dihedral pairs at 463 K from the quantum chemistry based RIS model are given in Figure 6, a and b, respectively. Not surprisingly, the g^+g^+ and g^-g^- sequences are the most populous, accounting for about 30% of the total population for $-\text{CH}_2-$ and $-\text{CF}_2-$ centered pairs. The pair population distribution is quite similar for the $-\text{CH}_2-$ and $-\text{CF}_2-$ centered pairs with the exception of the t_+t_+ and t_-t_- sequences. While this population is low in both cases, the population is about 3 times greater for the $-\text{CF}_2-$ centered pairs. The total gauche population of the backbone dihedrals in PVDF is 65%.

Comparison with Previous PVDF RIS Models.

The current model differs fundamentally from the previous six-state model for PVDF¹⁷ in that the distorted gauche states are considered to be manifested only as the result of pentane interactions and are not true independent split states, as in t_- and t_+ . The three-state model¹⁶ does not consider split conformations. In both models energies for first-order and second-order interac-

tions were estimated from molecular mechanics calculations and were adjusted so that RIS predictions for C_∞ agree with experiment. In contrast, our quantum chemistry based force field yields a reasonable value for C_∞ without empirical adjustments. While predictions for C_∞ are similar for the three models ($C_\infty = 6.43$ from ref 16 and $C_\infty = 5.5$ from ref 17), the previous models yield conformational populations that differ significantly from the quantum chemistry based model. The six-state¹⁷ and three-state¹⁶ models yield a gauche fraction of 47% and 51% at 463 K, respectively, compared with 65% for our model. The preference of the previous models for trans conformations is further demonstrated by comparing the energies predicted by the three-state model¹⁶ for the HPH conformers, shown in Table 5, with those obtained from quantum chemistry and those yielded by the present model. The predicted energies differ qualitatively from those obtained from quantum chemistry and subsequently accurately produced by the present RIS model.

The compact nature of the PVDF coil can be attributed to the high gauche fraction in the current model. In the three-state model, the chains are compact due to the relatively large population of g^+g^- type "hairpin" conformations, which greatly reduce the size of the polymer coil. At 463 K, the three-state model¹⁶ yields a population of 10.5% for $-\text{CH}_2-$ centered hairpins and 7.5% for $-\text{CF}_2-$ centered hairpins, while our model predicts a population of 2.4% for the $-\text{CH}_2-$ centered hairpins and 2.8% for the $-\text{CF}_2-$ centered hairpins. For the six-state model, the compact nature of the PVDF coil is attributable in part to the smaller values employed for the backbone valence angles.

Comparison of PVDF, PE, and PTFE. The characteristic ratio of PVDF from the current RIS model is compared with that of PE¹⁴ and PTFE¹¹ in Figure 5. At 463 K, PVDF is more compact than both PE and PTFE, and its characteristic ratio exhibits a much weaker dependence on temperature. The relative compactness of PVDF can be largely attributed to its high (65%) gauche fraction compared to PE (48%) and PTFE (30%).²⁰ The large negative temperature dependence of the characteristic ratios in PE and PTFE is due to an increase in gauche fraction and hairpin conformations with increasing temperature. While the latter increases in PVDF with increasing temperature, the gauche fraction is nearly independent of temperature, resulting in a much reduced temperature dependence of the characteristic ratio.

Conclusions

On the basis of high-level quantum chemistry calculations on model compounds, we have developed a picture for the conformational geometries and energies of PVDF that differs fundamental from those previously presented. Quantum chemistry reveals that while the trans state splits in PVDF model compounds, the gauche states do not. Rotational isomeric state analysis of the conformational energetics of the PVDF model compounds reveals an intrinsic preference for the trans state. However, strong unfavorable second-order effects in $-\text{CH}_2-$ centered dihedral pairs greatly suppress the trans population. As a result, and in stark contrast to predictions of previous RIS models, PVDF is found to have a high gauche fraction of dihedrals, resulting in relatively compact random coil compared to polyethylene and poly(tetrafluoroethylene).

Acknowledgment. This research is funded in part by the University of Utah Center for the Simulation of Accidental Fires and Explosions (C-SAFE), funded by the Department of Energy, Lawrence Livermore National Laboratory, under Subcontract B341493.

References and Notes

- (1) For a comprehensive review of the properties of PVDF, see: Lovinger, A. J. Poly(vinylidene Fluoride). In *Developments in Crystalline Polymers-I*; Bassett, D. C., Ed.; *Appl. Sci.* **1982**, 195-273.
- (2) Hasegawa, R.; Takashi, Ya.; Chatani, Yo.; Tadokoro, H. *Polym. J.* **1972**, 3, 600.
- (3) Takashi, Y.; Tadokoro, H. *Macromolecules* **1980**, 13, 1317.
- (4) Takashi, Y.; Matsubara, Y.; Tadokoro, H. *Macromolecules* **1983**, 16, 1588.
- (5) Lovinger, A. J. *Macromolecules* **1981**, 14, 322.
- (6) Kawai, H. *Jpn. J. Appl. Phys.* **1969**, 8, 975.
- (7) Bergman, J. G.; McFee, J. H.; Crane, G. R. *Appl. Phys. Lett.* **1971**, 18, 203.
- (8) Harnischfeger, P.; Jungnickel, B. *J. Appl. Phys.* **1990**, A50, 523.
- (9) Wang, T. T.; Herbert, J. M.; Glass, A. M., Eds. *The Application of Ferroelectric Polymers*; Chapman and Hall: New York, 1987.
- (10) Frisch, M. J.; Trucks, G. W.; Schlegel, H. B.; Scuseria, G. E.; Robb, M. A.; Cheeseman, J. R.; Zakrzewski, V. G.; Montgomery, J. A., Jr.; Stratmann, R. E.; Burant, J. C.; Dapprich, S.; Millam, J. M.; Daniels, A. D.; Kudin, K. N.; Strain, M. C.; Farkas, O.; Tomasi, J.; Barone, V.; Cossi, M.; Cammi, R.; Mennucci, B.; Pomelli, C.; Adamo, C.; Clifford, S.; Ochterski, J.; Petersson, G. A.; Ayala, J. Y.; Cui, Q.; Morokuma, K.; Malick, D. K.; Rabuck, A. D.; Raghavachari, K.; Foresman, J. B.; Cioslowski, J.; Ortiz, J. V.; Stefanov, B. B.; Liu, G.; Liashenko, A.; Piskorz, P.; Komaromi, I.; Gomperts, R.; Martin, R. L.; Fox, D. J.; Keith, T.; Al-Laham, M. A.; Peng, C. Y.; Nanayakkara, A.; Gonzalez, C.; Challacombe, M.; Gill, P. M. W.; Johnson, B.; Chen, A.; Wong, M. W.; Andres, J. L.; Gonzalez, C.; Head-Gordon, M.; Replogle, E. S.; Pople, J. A. *Gaussian 98, Revision A.1*; Gaussian, Inc.: Pittsburgh, PA, 1998.
- (11) Smith, G. D.; Jaffe, R. L.; Yoon, D. Y. *Macromolecules* **1994**, 27, 3166.
- (12) Smith, G. D.; Jaffe, R. L.; Yoon, D. Y. *Macromolecules* **1995**, 28, 5804.
- (13) Karasawa, N.; Goddard, W. A., III *Macromolecules* **1992**, 25, 7268.
- (14) Boyd, R. H.; Breitling, S. M. *Macromolecules* **1972**, 5, 279.
- (15) Abe, A.; Jernigan, R. L.; Flory, P. J. *J. Am. Chem. Soc.* **1966**, 88, 631.
- (16) Tonelli, A. E. *Macromolecules* **1976**, 9, 547.
- (17) Mattice, W. L.; Suter, U. W. *Conformational Theory of Large Molecules*; John Wiley & Sons: New York, 1994. Carballreira, L.; Pereiras, A. J.; Rios, M. A. *Macromolecules* **1990**, 23, 1309.
- (18) Flory, P. J. *Statistical Mechanics of Chain Molecules*; Interscience: New York, 1969.
- (19) Welch, G. J. *Polymer* **1974**, 15, 429.
- (20) Chu, B.; Wu, C.; Buck, W. *Macromolecules* **1989**, 22, 831.

MA9902605